NANO LETTERS

2005
Vol. 5, No. 11
2160−2163

Photothermal Absorption Spectroscopy of Individual Semiconductor Nanocrystals

Stéphane Berciaud, Laurent Cognet, and Brahim Lounis*

Centre de Physique Moléculaire Optique et Hertzienne, CNRS (UMR 5798) et Université Bordeaux I, 351, cours de la Libération, 33405 Talence Cedex, France

Received September 8, 2005; Revised Manuscript Received October 11, 2005

ABSTRACT

Photothermal heterodyne detection is used to record the first room-temperature absorption spectra of single CdSe/ZnS semiconductor nanocrystals. These spectra are recorded in the high cw excitation regime, and the observed bands are assigned to transitions involving biexciton and trion states. Comparison with the single nanocrystals photoluminescence spectra leads to the measurement of spectral Stokes shifts free from ensemble averaging.

Core-shell CdSe/ZnS semiconductor nanocrystals exhibit unique size-dependent optical properties,[1] which make them ideal candidates for applications in various fields such as the design of new optical devices[1−3] or biolabeling.[4] For full exploitation, understanding of their optical properties is, however, crucial. Ensemble photoluminescence and linear absorption measurements provided a comprehensive description of the excitonic levels structure of CdSe/ZnS nanocrystals[5] and allowed for a precise assignment of the optical transitions.[6] Individual nanocrystals are now detected commonly using standard fluorescence microscopes with low excitation intensities because of the high radiative quantum yield of their band-edge exciton state X ($1S_e$, $1S_{h,3/2}$) (see ref 6 for spectroscopic notations). Their luminescence displays a blinking[7] behavior with intensity-dependent on-time distributions and strong photon antibunching.[8,9]

CdSe/ZnS nanocrystals have relatively high absorption cross-sections[8,10] (typically $\sim 10^{-15}$ cm^2) and when excited with sufficiently high intensities, excitons are created at average rates, N_{abs}, significantly higher than their radiative recombination rates, Γ_{rad}.[8,11] In this regime, efficient nonradiative Auger recombinations of the prepared multiexcitons take place.[12] In CdSe/ZnS nanocrystals, these recombinations occur in the picosecond range as measured in time-resolved experiments on ensemble samples.[13] Individual nanocrystals could thus be detected through their absorption using the photothermal heterodyne method.[14]

Although recording the luminescence spectra from single nanocrystals has become routine, a measurement of the absorption spectra of individual nanocrystals has, however, never been reported because of a lack of sensitive enough methods. In this letter, we present the first room-temperature photothermal absorption spectra of individual nanocrystals.

In the photothermal techniques,[14,15] the signal is proportional to the amount of laser power absorbed by a single nanoparticle converted into heat by nonradiative relaxation processes. This allowed us to detect individual tiny metal nanoparticles and to perform spectroscopy of their Plasmon resonance.[16] For nanocrystals, the signal has its origin from two possible nonradiative relaxation pathways. First, at the high cw excitation rates required in the photothermal method (typically $N_{abs} \approx 1$ ns^{-1}), biexcitons are created in the nanocrystal and the ($1S_e$, $1S_{h,3/2}$) ($1S_e$, $1S_{h,3/2}$) biexciton state (XX) is prepared. A rapid recombination of one of the two excitons through Auger processes occurs ($\Gamma_{XX} > 20$ ns^{-1} for 2 nm nanocrystals[13]) and is followed by a nonradiative relaxation of the remaining exciton to the band-edge state, X. Because N_{abs} is much higher than Γ_{rad} ($\sim$1/20 ns^{-1}), multiexciton creation prevents radiative recombination of the monoexcitons efficiently. Thus, the first contribution to the signal arises from continuous cycling of the nanocrystal between the band-edge, X, and biexciton, XX, states (see Figure 1). The second mechanism contributing to the signal comes into play when the nanocrystal is in a charged state. It is known that continuous excitation of a CdSe nanocrystal can lead to a spontaneous or Auger-type ejection of charges to the shell or to the local environment of the nanocrystal.[7,17,18] In this case, absorption leads to the formation of trions and the photothermal signal arises from fast Auger nonradiative recombination of the X* state to the ground charge state, 0* ($\Gamma_{X^*} \approx 20$ ns^{-1}).[19] In addition, with our experimental parameters the probability to prepare triexcitons from XX or charged biexcitons from X* is very low ($N_{abs} \ll \Gamma_{XX}$, Γ_{X^*}).

The absorption spectroscopy setup (Figure 2) using photothermal heterodyne signals was described elsewhere.[16] In

* Corresponding author. E-mail: b.lounis@cpmoh.u-bordeaux1.fr.

10.1021/nl051805d CCC: $30.25 © 2005 American Chemical Society
Published on Web 10/25/2005

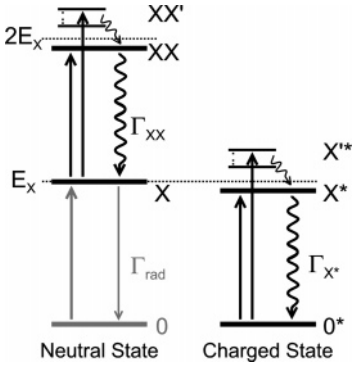

Figure 1. Energy diagram of the excitonic states involved in the photothermal signal from nanocrystals in the neutral and charged state. For notations see details in the text.

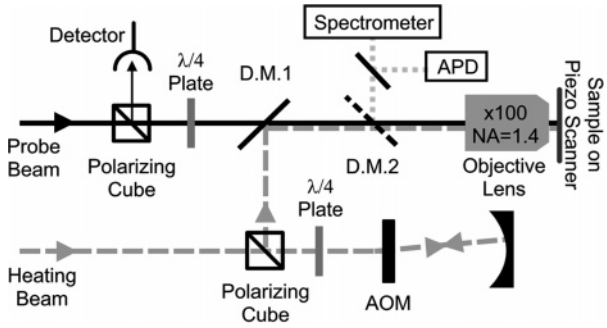

Figure 2. Schematic of the experimental setup.

short, it consists of a heating beam (tunable cw dye laser, Coherent 599, tuning range 530−590 nm corresponding to photon energies of 2.10−2.34 eV) overlaid with a probe beam (HeNe laser, 633 nm wavelength, well below the band-edge absorption of the nanocrystals). The heating beam is circularly polarized with an intensity of ∼1 MW/cm^2 corresponding to absorption rates of $N_{abs} \approx 1$ ns^{-1}. Both beams are focused on the sample using a high NA objective. A fluorescence confocal microscopy scheme is also implemented on this setup. It is used to image individual luminescent nanocrystals and to record their luminescence spectra. For these measurements, the heating laser is used for the excitation with an attenuated intensity (∼1 kW/cm^2) and a fixed energy (2.30 eV). The collected luminescence photons are split toward an avalanche photodiode and a spectrometer. The samples were prepared by spin-coating dilute solutions of nanocrystals (QDot 585 Steptavidin conjugate average radius: 2.0 nm, peak emission at ∼2.10 eV, dissolved in 1% mass polyvinyl−alcohol aqueous solution) onto clean microscope coverslips. The dilution and spinning rates were chosen such that the final density of nanoparticles in the samples is less than 1 μm^{-2}. A drop of viscous silicon oil was added on top of the samples to ensure homogeneity of heat diffusion.

Individual fluorescent nanocrystals were first located by recording a 20 × 20 μm^2 fluorescence image of the sample (Figure 3a). For each spot, a luminescence time trace and

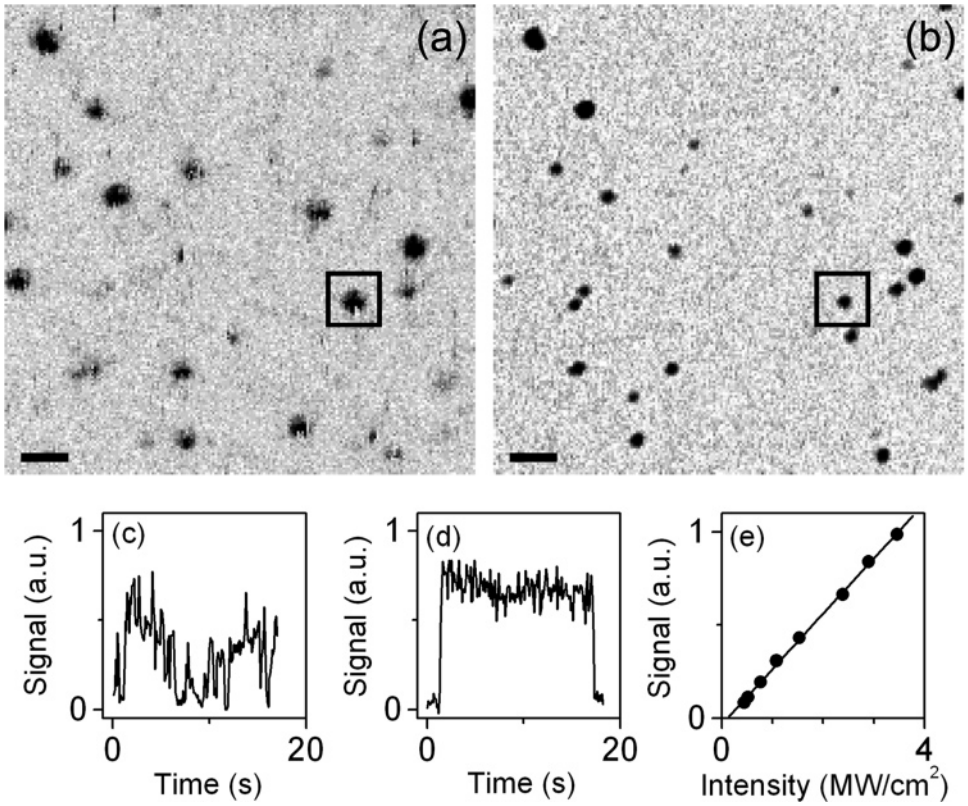

Figure 3. (a) Comparison of photoluminescence and (b) photothermal heterodyne images of the same area 20 × 20 μm^2 of a sample containing CdSe/ZnS nanocrystals. The integration time per point was 10 ms. Scale bar is 2 μm. Photoluminescence (c) and photothermal (d) signals recorded over time for the individual nanocrystal highlighted on a and b. The integration time per point was 100 ms. (e) Photothermal signal obtained from an individual nanocrystal (circles) as a function of the heating intensity. The heating photon energy was 2.30 eV. The data are adjusted by a linear fit (solid line).

an emission spectrum were recorded simultaneously. The blinking behavior, a signature of single nanocrystal emission, is clearly visible in the time trace shown in Figure 3c. We then recorded a photothermal image of the same sample area (Figure 3b). Clearly the luminescence and photothermal images correlate well (>80% of the luminescence spots correlate with a photothermal spot), proving that the spots in the photothermal image stem from individual nanocrystals. Contrary to luminescence, the photothermal signals do not show any blinking behavior (Figure 3d). They remain stable during time scales larger than those necessary to record an absorption spectrum.

As expected, we observe a large heterogeneity of luminescence spot heights because of diversity in nanocrystal structures, surface states, and orientations with the respect to the polarization of the excitation light. As can be seen in Figure 3b, the photothermal signal levels recorded from individual nanocrystals are also heterogeneous. However, we cannot establish a clear correlation between the heterogeneities of the luminescence and photothermal signal levels. We also notice that some nonluminescent nanocrystals (which do not appear in Figure 3a) are observed on the photothermal image. Furthermore, the photothermal signal scales linearly with the heating intensity (Figure 3e) because the transitions involved in the signal are not saturated ($N_{abs} \ll \Gamma_{XX}, \Gamma_{X*}$).

We acquired the photothermal absorption spectra for the nanocrystals that colocalize in the luminescence and photothermal images. Figure 4 (top) presents the results obtained from the individual nanocrystal highlighted in Figure 3. For the absorption spectrum, the laser frequency was scanned with steps of 4 meV and 200 ms integration times per point. The signals are corrected for the wavelength dependence of the diffraction-limited laser spot size, and the heating power at the sample was measured during the acquisitions for normalization.

Contrary to the ensemble luminescence spectrum, which has an inhomogeneously broadened Gaussian shape (open circles of Figure 4 (bottom) with peak energy at 2.100 eV and full-width-at-half-maximum (FWHM) of 100 meV), the luminescence spectrum displays a narrower homogeneous Lorentzian shape peaked at 2.120 eV and a FWHM of 65 meV (open circles in Figure 4 (top)). The absorption spectrum of the same nanocrystal (measured with the photothermal method) and that of an ensemble of nanocrystals (measured with a spectrophotometer) are also shown on Figure 4 (solid lines). Both of them contain a first absorption peak at, respectively, 2.160 and 2.170 eV, blue shifted from the emission lines. Similar to the emission spectrum, the width of the single nanocrystal absorption peak is narrower than that of the ensemble. The two peaks of the ensemble absorption spectrum, recorded in the weak excitation regime, are assigned to the band-edge X state and to the higher energy ($1S_e$, $2S_{h,3/2}$) state[6,20] (Figure 4 (bottom, solid line)). The nonresonant Stokes shift ΔE_S is defined as the energy difference between the first absorption peak and the luminescence maximum energy. We found $\Delta E_S \approx 70$ meV, in agreement with previous ensemble studies.[21]

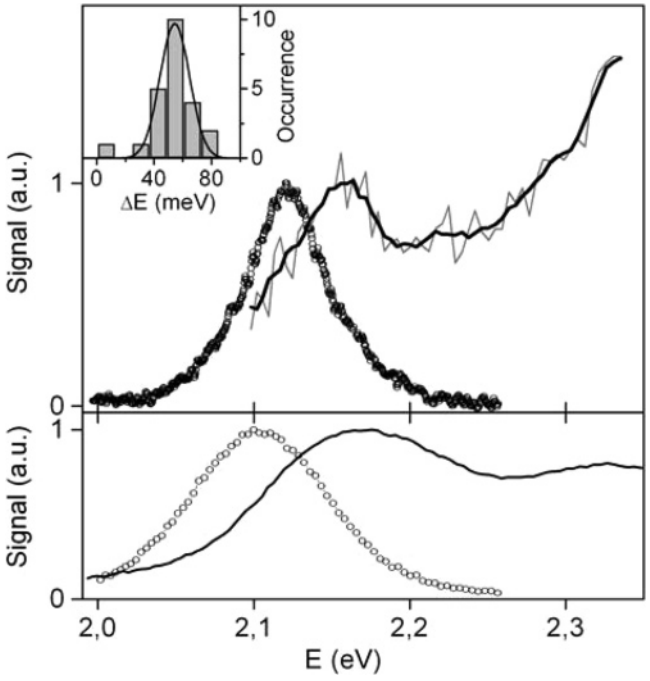

Figure 4. Top: photoluminescence (open circles) and photothermal absorption (solid lines) spectra recorded for the individual nanocrystal highlighted in Figure 3. For clarity, a smoothing of the absorption spectra is shown. Bottom: photoluminescence (open circles) and linear absorption spectra (solid line) of an ensemble of nanocrystals. Inset: histogram of the values of ΔE obtained from photoluminescence and photothermal absorption spectra of 23 individual nanocrystals. The distribution is fitted by a Gaussian curve (black line).

The photothermal absorption spectrum presented in Figure 4 (top, solid line) exhibits one clear band and a rising feature at higher energies that is not fully scanned because of insufficient laser tuning range. We assign the low energy band to the two unresolved X → XX and 0* → X* transitions. Indeed, Coulomb interactions induce comparable red-shifts of the transitions[22] with respect to E_X, the energy of the 0 → X transition (see Figure 1). The rising feature in the spectrum may involve X → XX′ and 0* → X′* transitions where X′ denotes a high energy exciton state (such as ($1S_e$, $2S_{h,3/2}$) or ($1P_e$, $1P_{h,3/2}$)).

We performed the same measurements for 23 individual nanocrystals and observed qualitatively comparable spectra. For each of them, we extracted the energy separation, ΔE, between the position of the low energy absorption band and the luminescence peak. The histogram of the values of ΔE is shown in Figure 4 (inset). It is well fitted by a Gaussian distribution with a FWHM of 12 mV and a mean value of ~50 meV smaller by ~20 meV than ΔE_S. This deviation is in agreement with the values of biexciton and trion binding energies deduced from femtosecond photoluminescence upconversion[23] and transient photoluminescence[24] studies (~20−30 meV for a 2 nm nanocrystal) as well as from the emission properties of single colloidal nanocrystals[25] or self-assembled quantum dots[22] in charged states.

In conclusion, we have demonstrated the applicability of the photothermal heterodyne method to room-temperature detection and absorption spectroscopy of individual CdSe/

ZnS semiconductor nanocrystals in the multiexcitonic regime. We foresee promising spectroscopic studies of nanocrystals using this method with samples at cryogenic temperatures. For example, it would be interesting to compare low-temperature photothermal absorption spectra to the recent results on photoluminescence excitation spectroscopy of single nanocrystals,[26] which support the existence of an energy "minigap" separating the discrete band-edge excitonic levels from a quasicontinuum.

Acknowledgment. We thank O. Labeau, P. Tamarat, and G. Blab for helpful discussions and A. L. Efros for the reading of the manuscript. This research was funded by CNRS (ACI Nanoscience and DRAB), Région Aquitaine and the French Ministry for Education and Research (MENRT).

References

(1) Klimov, V. I. *Semiconductor and Metal Nanocrystals: Synthesis, Electronic and Optical Properties*; Marcel Dekker: New York, 2003.
(2) Colvin, V. L.; Schlamp, M. C.; Alivisatos, A. P. *Nature* **1994**, *370*, 354−357.
(3) Dabbousi, B. O.; Bawendi, M. G.; Onitsuka, O.; Rubner, M. F. *Appl. Phys. Lett.* **1995**, *66*, 1316−18.
(4) Chan, W. C.; Maxwell, D. J.; Gao, X.; Bailey, R. E.; Han, M.; Nie, S. *Curr. Opin. Biotechnol.* **2002**, *13*, 40−6.
(5) Efros, A. L.; Rosen, M.; Kuno, M.; Nirmal, M.; Norris, D. J.; Bawendi, M. *Phys. Rev. B: Condens. Matter* **1996**, *54*, 4843−4856.
(6) Norris, D. J.; Bawendi, M. G. *Phys. Rev. B: Condens. Matter* **1996**, *53*, 16338−16346.
(7) Nirmal, M.; Dabbousi, B. O.; Bawendi, M. G.; Macklin, J. J.; Trautman, J. K.; Harris, T. D.; Brus, L. E. *Nature* **1996**, *383*, 802−804.
(8) Lounis, B.; Bechtel, H. A.; Gerion, D.; Alivisatos, A. P.; Moerner, W. E. *Chem. Phys. Lett.* **2000**, *329*, 399.
(9) Michler, P.; Imamoglu, A.; Mason, M. D.; Carson, P. J.; Strouse, G. F.; Buratto, S. K. *Nature* **2000**, *406*, 968−70.
(10) Leatherdale, C. A.; Woo, W.-K.; Mikulec, F. V.; Bawendi, M. G. *J. Phys. Chem. B* **2002**, *106*, 7619.
(11) Schlegel, G.; Bohnenberger, J.; Potapova, I.; Mews, A. *Phys. Rev. Lett.* **2002**, *88*, 137401.
(12) Efros, A. L.; Lockwood, D. J.; Tsybeskov, L. *Semiconductor Nanocrystals*; Kluwer Academic/Plenum Publishers: New York, 2003.
(13) Klimov, V. I.; Mikhailovsky, A. A.; McBranch, D. W.; Leatherdale, C. A.; Bawendi, M. G. *Science* **2000**, *287*, 1011−3.
(14) Berciaud, S.; Cognet, L.; Blab, G. A.; Lounis, B. *Phys. Rev. Lett.* **2004**, *93*, 257402.
(15) Boyer, D.; Tamarat, P.; Maali, A.; Lounis, B.; Orrit, M. *Science* **2002**, *297*, 1160−1163.
(16) Berciaud, S.; Cognet, L.; Tamarat, P.; Lounis, B. *Nano Lett.* **2005**, *5*, 515−518.
(17) Efros, A. L.; Rosen, M. *Phys. Rev. Lett.* **1997**, *78*, 1110−1113.
(18) Krauss, T. D.; O'Brien, S.; Brus, L. E. *J. Phys. Chem. B* **2001**, *105*, 1725−1733.
(19) Wang, L. W.; Califano, M.; Zunger, A.; Franceschetti, A. *Phys. Rev. Lett.* **2003**, *91*, 056404.
(20) Ekimov, A. I.; Hache, F.; Schanne-Klein, M. C.; Ricard, D.; Flytzanis, C.; Kudryavtsev, I. A.; Yazeva, T. V.; Rodina, A. V.; Efros, A. L. *J. Opt. Soc. Am. B* **1993**, *10*, 100−107.
(21) Kuno, M.; Lee, J. K.; Dabbousi, B. O.; Mikulec, F. V.; Bawendi, M. G. T *J. Chem. Phys.* **1997**, *106*, 9869.
(22) Patton, B.; Langbein, W.; Woggon, U. *Phys. Rev. B* **2003**, *68*, 125316.
(23) Achermann, M.; Hollingsworth, J. A.; Klimov, V. I. *Phys. Rev. B* **2003**, *68*, 245302.
(24) Caruge, J. M.; Chan, Y.; Sundar, V.; Eisler, H. J.; Bawendi, M. G. *Phys. Rev. B* **2004**, *70*, 085316.
(25) Shimizu, K. T.; Woo, W. K.; Fisher, B. R.; Eisler, H. J.; Bawendi, M. G. *Phys. Rev. Lett.* **2002**, *89*, 117401.
(26) Htoon, H.; Cox, P. J.; Klimov, V. I. *Phys. Rev. Lett.* **2004**, *93*, 187402.

NL051805D